Biochemical Pharmacology 80 (2010) 335–343

Contents lists available at ScienceDirect

Biochemical Pharmacology

journal homepage: www.elsevier.com/locate/biochempharm

The NER proteins XPC and CSB, but not ERCC1, regulate the sensitivity to the novel DNA binder S23906: Implications for recognition and repair of antitumor alkylators

Céline J. Rocca [a,b,c], Virginie Poindessous [a,b,c], Daniele G. Soares [a,b,c,d], Karima El Ouadrani [a,b,c], Alain Sarasin [e,f], Eric Guérin [g,h], Aimery de Gramont [a,b,c,i], João A.P. Henriques [d], Alexandre E. Escargueil [a,b,c], Annette K. Larsen [a,b,c,*]

[a] Laboratory of Cancer Biology and Therapeutics, Centre de Recherche Saint-Antoine, Paris 75571, France
[b] Institut National de la Santé et de la Recherche Médicale U938, Paris, France
[c] Université Pierre et Marie Curie (Univ. Paris 6), Paris, France
[d] Departamento de Biofísica/Centro de Biotecnologia, Universidade Federal do Rio Grande do Sul, Porto Alegre, Brazil
[e] Centre National de la Recherche Scientifique FRE 2939, Villejuif, France
[f] Institut Gustave-Roussy, 94805 Villejuif, France
[g] Laboratoire de Biochimie et Biologie Moléculaire, Hôpital de Hautepierre, Strasbourg, France
[h] Université de Strasbourg, Equipe d'Accueil 4438 Physiopathologie et Médecine Translationnelle. 67081 Strasbourg, France
[i] Department of Clinical Oncology, Hôpital Saint-Antoine, AP-HP, Paris 75571, France

ARTICLE INFO

Article history:
Received 17 February 2010
Accepted 9 April 2010

Keywords:
Nucleotide excision repair
S23906
Monofunctional alkylators
XPC
ERCC1

ABSTRACT

S23906 belongs to a novel class of alkylating anticancer agents forming bulky monofunctional DNA adducts. A unique feature of S23906 is its "helicase-like" activity leading to the destabilization of the surrounding duplex DNA. We here characterize the recognition and repair of S23906 adducts by the nucleotide excision repair (NER) machinery. All NER-deficient human cell lines tested showed increased sensitivity to S23906, which was particularly pronounced for cells deficient in XPC, CSB and XPA. In comparison, deficiencies in ERCC1 or XPF had lesser impact on the sensitivity to S23906. The sensitivity was, at least in part, linked to the conversion of unrepaired adducts into toxic DNA strand breaks as shown by single cell electrophoresis and gamma-H2AX formation. The pharmacological relevance of these findings was confirmed by the characterization of KB carcinoma cells with acquired S23906 resistance. These cells showed increased NER activity *in vivo* as well as toward damaged plasmid DNA *in vitro*. In particular, both global genome NER, as shown by unscheduled DNA synthesis, and transcription-coupled NER, as shown by transcriptional recovery, were up-regulated in the S23906-resistant cells. The increased NER activity was accompanied by up to 5-fold up-regulation of XPC, CSB and XPA proteins without detectable alterations of ERCC1 on the DNA, RNA or protein levels. Our results suggest that S23906 adducts are recognized and repaired by both NER sub-pathways in contrast to other members of this class, that are only recognized by transcription-coupled NER. We further show that NER activity can be up-regulated without changes in ERCC1 expression.

1. Introduction

DNA targeted agents have proven clinical activity toward most human cancers and remain the mainstay of cancer chemotherapeutic regimens. However, additional drugs with novel mechanisms of action and/or different activities are needed. A promising class of DNA targeted agents is characterized by the formation of bulky monofunctional adducts, and one such compound, yondelis/tranbectedin was recently approved for clinical use in Europe. A particularly interesting feature of this class of agents is their capacity to modulate local chromatin structure. For example, yondelis forms covalent adducts with guanine in the minor groove of DNA that result in pronounced stabilization of the neighboring duplex structure [1].

S23906 is an acronycine derivative which forms bulky adducts with the exocyclic amino group of guanine residues in the minor groove of DNA [2,3]. A unique property of S23906, compared to other anticancer agents, is its "helicase-like" activity which leads

* Corresponding author at: Laboratory of Cancer Biology and Therapeutics, Hôpital Saint-Antoine, Kourilsky Building 1st floor, 184 rue du Faubourg Saint-Antoine, 75571 Paris Cedex 12, France. Tel.: +331 49 28 46 12; fax: +331 42 22 64 29.
E-mail address: akraghlarsen@aol.com (A.K. Larsen).

0006-2952/$ – see front matter © 2010 Elsevier Inc. All rights reserved.
doi:10.1016/j.bcp.2010.04.012

to the destabilization of the duplex structure in the vicinity of the adducts thereby facilitating base unpairing and helix opening [1]. Thus, although yondelis and S23906 target the same DNA residues, their influence on local chromatin structure are completely different. Both types of adducts can be converted into DNA double strand breaks (DSBs) by collision with the replication fork and may be accompanied by mitotic catastrophe [4–6].

Nucleotide excision repair (NER) is one of our most versatile repair pathways in terms of lesion recognition and influences the response to many DNA binding agents [7]. Recognition of DNA damage can occur either by global genome repair (GG-NER), that removes DNA damage from the entire genome, or by transcription-coupled repair (TC-NER), that preferentially repairs the transcribed strand of actively expressed genes. Both processes are essentially similar except for the initial damage recognition step that is performed by XPC-hHR23B in GG-NER and by the stalled RNA polymerase II complex in TC-NER. Transcription-coupled repair also requires Cockayne's syndrome-related factors CSA and CSB. Then, the transcription/repair factor IIH is recruited for strand separation which is mediated by the helicase activity of XPD followed by the recruitment of the XPA protein. Incision on each site of the lesion is carried out by the endonucleases XPG and ERCC1–XPF, which is the last step in the NER process. The generated gap is subsequently filled by DNA repair synthesis [8–10].

Recently, large clinical trials have been undertaken to establish if expression levels of the ERCC1 protein in patient tumors can predict the response to platinum treatment [11]. The results are encouraging provided the methodological issues can be resolved [12]. In comparison, previous studies have revealed a complex interaction between the bulky monofunctional alkylators and the NER machinery. For example, irofulven is an excellent substrate for TC-NER but is not recognized by GG-NER [13–16]. Furthermore, the activity of irofulven toward a large tumor cell panel was closely correlated with the expression of the XPG endonuclease, but not with ERCC1 or XPF [14]. In a similar manner, yondelis is recognized by TC-NER, but not by GG-NER [17]. However, in this case, the yondelis adducts are not removed, but rather converted into more toxic repair intermediates, most likely due to the formation of stable complexes between the yondelis adducts and the XPG endonuclease [18].

We here describe the interaction between S23906 and the NER pathway. Human cells deficient for XPC, CSB and XPA showed pronounced sensitivity to S23906, whereas deficiencies in ERCC1 and XPF played lesser roles. The pharmacological relevance of these findings was further confirmed by the characterization of tumor cells with acquired S23906 resistance. These cells showed increased NER activity and up to 5-fold up-regulation of XPC, CSB and XPA proteins, but no detectable alterations in ERCC1. Our results underline the unusual interactions between the bulky monofunctional alkylators and the NER machinery and strongly suggest that NER activity can be up-regulated independently of ERCC1.

2. Materials and methods

2.1. Chemicals

The acronycine derivative S23906 (cis-1,2-diacetoxy-3,14-dihydro-3,3,14-trimethyl-6-methoxy-7H-benz[b]pyrano[3,2-d]acridin-7-one) was obtained from Institut de Recherches Servier (Croissy sur Seine, France) while cisplatin was purchased from Merck Génériques (Lyon, France).

2.2. Cells

NER-deficient cell lines derived from unexposed skin biopsies of patients with *xeroderma pigmentosum* or Cockayne's syndrome were provided by Alain Sarasin (Villejuif, France), and included 198VI (wild type), MRC5-SV (wild type), XP162VI (XPA-deficient), XP12RO-SV (XPA-deficient), XP202VI (XPC-deficient), XP4PA-SV (XPC-deficient), SC1AN-SV (CSB-deficient), CS539VI (CSB-deficient), XPCS2BA-SV (XPB-deficient), XP6BE-SV (XPD-deficient), XPCS1LV (XPG-deficient) and XP871VI (XPF-deficient). An additional NER-deficient cell line, 165TOR (ERCC1-deficient) [19], was kindly provided by Jan Hoeijmakers (Rotterdam, the Netherlands). The genetic alterations in the XP and CS cells are listed in Table 1. KB parental and S23906-resistant KB/906 epidermoid carcinoma cells [4] were a gift from Alain Pierré (Croissy sur Seine, France).

2.3. Growth inhibition

Cells were exposed to the indicated concentrations of S23906 and cisplatin for 4–5 generation times followed by the determination of cellular viability by the MTT colorimetric assay as described previously [16]. Alternatively, cells were exposed to 0–30 J/m^2 of UV-C irradiation followed by post-incubation in drug-free media for 4–5 generation times and the MTT assay. Cells deficient in ERCC1 and XPF have low metabolic rates. Therefore, experiments with these cells were carried out in 12-well plates with 15,000 cells/well in 5 ml media rather than under standard conditions (24-well plates with 5000 cells/well in 2 ml media).

Table 1
Repair-proficient and -deficient cells used in this study.

Gene affected	Human fibroblast strain	Alternative name	Mutation
wt	198VI	AS198	
wt	MRC5-SV		
XPA	XP162VI	AS162	c.682 C>T homozygous; p.Arg228X
XPA	XP12RO-SV		c.619 C>T; p.R207X homozygous
XPB	XPCS2BA-SV		c.296 T>C; p.F99S (only one allele expressed)
XPC	XP202VI	AS202	c.1643_1644delTG homozygous; p.Val548AlafsX572
XPC	XP4PA-SV	XPC1	c.1643_1644delTG homozygous; p.Val548AlafsX572
XPD	XP6BE-SV	AS203	c.2047 C>T; p.R683W heterozygous and c.del106_183; p.del36_61
XPF[a]	XP871VI	AS871	R589W heterozygous and exon 3 deletion heterozygous
XPG	XPCS1LV		c.delA 2170; p.A659X homozygous
ERCC1		165TOR	C.472 C>T; p.Gln158X heterozygous C.691 C>G; p.Phe231Leu heterozygous
CSB	CS1AN-SV		c.1009A>T; p.Lys337X and c.2569C>T heterozygous; p.Tyr834CysfsX25 heterozygous
CSB	CS539VI	AS539	Promoter deletion; p. 0 homozygous

[a] K. Jaspers and A. Sarasin, unpublished data.

2.4. Unscheduled DNA synthesis (UDS)

Unscheduled DNA synthesis, which principally measures global genome NER activity, was carried out as described previously [14]. Briefly, growth-arrested cells were co-incubated with 10 μCi/ml [methyl-^{3}H]thymidine (TRK-686 1 mCi/ml, Amersham, Buckinghamshire, United Kingdom) and S23906 for 3 h or subjected to 254 nm UV-C irradiation followed by post-incubation with methyl-[^{3}H]thymidine. The number of grains, indicating UDS, was determined for at least 30 nuclei/sample for primary cell lines and 100 nuclei/sample for transformed cell lines. Results are averages of at least two independent experiments.

2.5. Single cell gel electrophoresis (comet assay)

XPA-proficient (MRC5-SV) and -deficient (XP12RO-SV) cells were exposed to the indicated drug concentrations for 1 h at 37 °C in the dark and subjected to single cell electrophoresis (comet assay) under alkaline conditions as described [20]. Image analysis was performed using Komet 5.5 software (Kinetic Imaging, Nottingham, UK) to determine the % of nuclear DNA present in the comet tail. At least 100 cells were analyzed per sample. Values represent the average of at least two independent experiments.

2.6. Immunofluorescence and microscopy

XPA-proficient (MRC5-SV) and -deficient (XP12RO-SV) cells were treated with the indicated concentrations of S23906 for 1 h and phosphorylated H2AX was revealed by immunocytochemistry with a γ-H2AX-directed antibody (05-636, Upstate Biotechnology, Millipore, Saint-Quentin en Yvelines, France) as described [5]. Fluorescence intensities were measured using the MetaMorph Software (Universal Imaging, Downingtown, PA) and the background fluorescence over non-cellular regions was subtracted. At least 100 cells were analyzed per sample. Values represent the average of at least two independent experiments.

2.7. ERCC1 recruitment

KB and KB/906 cells were plated on coverslips, covered by 5 μm MCE membranes (Fisher Scientific, Illkirch, France) and submitted to local UV irradiation as described. [8]. UV-induced pyrimidine 6-4 pyrimidone photoproducts (6-4PPs) were detected with mouse monoclonal anti-6-4PPs antibodies (64M-2) as described [21] while ERCC1 was revealed by a polyclonal rabbit anti-ERCC1 antibody (sc10785, clone FL-297, Santa Cruz Biotechnology, Saint-Quentin, France). Secondary antibodies were Cy3-conjugated donkey anti-mouse IgG antibody (715-165-151; Jackson ImmunoResearch Laboratories, Bar Harbor, ME) and Alexa488-conjugated goat anti-rabbit IgG antibody (111-485-003; Jackson ImmunoResearch Laboratories).

2.8. 3D assay

The DNA damage detection assay (3D) measures *in vitro* DNA repair synthesis of UV adducts by cellular extracts and was carried out according to previously published procedures [22]. Briefly, cellular extracts were incubated with UV-irradiated plasmid DNA in the presence of dNTPs digoxigenylated deoxynucleotide monophosphates for 30 min and the incorporated nucleotides were quantified by chemiluminescence by an anti-DIG antibody conjugated with alkaline phosphatase (Roche, Meylan, France).

2.9. Transcriptional recovery

The transcriptional recovery of UV-irradiated KB and KB/906 cells was carried out according to previously published procedures [15] with minor modifications. Briefly, cells were UV-irradiated and the transcriptional recovery was estimated by the incorporation of 5 μCi/ml [5-^{3}H]uridine (TRK-178, 1 mCi/ml, Amersham) for 30 min. Cells were treated with trichloroacetic acid, loaded on GF/C filters (Whatman, Brentford, UK) and the radioactivity was determined by scintillation counting. The percentage of RNA synthesis is indicated as the ratio of treated/untreated cells.

2.10. Relative quantitative PCR (qRT-PCR analysis)

Expression levels of selected genes were measured by qRT-PCR as described previously [23]. The following validated primers were obtained from Qiagen (Courtaboeuf, France): XPC (QT00080381), CSB (QT00025732), XPA (QT01666133), XPD (QT00086758), XPB (QT00080276), XPG (QT00029246), XPF (QT00063091), ERCC1 (QT00059374), HMBS/PBGD (QT00014462), β-actin (QT00095431) and GAPDH (QT01192646). All quantifications were carried out in duplicate for two independent RNA extractions and normalized using the geometric mean of the three references genes (HMBS/PBGD, beta-actin and GAPDH) as recommended [24]. The corresponding amplimer samples were run on 2% agarose gel and PCR products were visualized by ethidium bromide staining.

2.11. Western blotting

Western blot analysis was carried out as described previously [15]. Expression of NER proteins was revealed using the following antibodies: polyclonal rabbit anti-ERCC1 (sc10785, clone FL-297, Santa Cruz Biotechnology), polyclonal goat anti-CSB (sc10459, clone E-18, Santa Cruz Biotechnology), polyclonal rabbit anti-XPC (ab21078, Abcam, Cambridge, UK) and polyclonal rabbit anti-XPA (sc853, clone FL-273, Santa Cruz Biotechnology) while actin was detected by monoclonal mouse anti-β-actin (A5441, clone AC-15, Sigma, Saint-Quentin Fallavier, France). The secondary antibodies included horseradish peroxidase-conjugated donkey anti-goat, horseradish peroxidase-conjugated donkey anti-rabbit and horseradish peroxidase-conjugated donkey anti-mouse (references 705-035-003, 711-035-152 and 715-035-150; Jackson ImmunoResearch Laboratories).

2.12. ERCC1 codon 118 polymorphism

Amplification of the DNA region encompassing codon 3 was carried out by PCR using the following primers: ECC1Ex3: TGTGGTTATCAAGGGTCATCCC and ERCC1Ex3R: CATGCCCAGAGGCTTCTCATAG. Two independent PCR reactions were carried out for each cell line followed by sequencing in both directions.

3. Results

3.1. Cytotoxicity of S23906 toward NER-deficient cells

To determine the impact of nucleotide excision repair, we determined the cytotoxicity of S23906 toward repair-proficient and XPA-deficient cells that are deficient in both the global genome and the transcription-coupled NER sub-pathways. Unexpectedly, XPA deficiency was accompanied by almost 45-fold increased sensitivity to S23906, compared to repair-proficient cells (Fig. 1A, diamonds). To determine if these results were specific for immortalized cell lines, similar experiments were carried out for

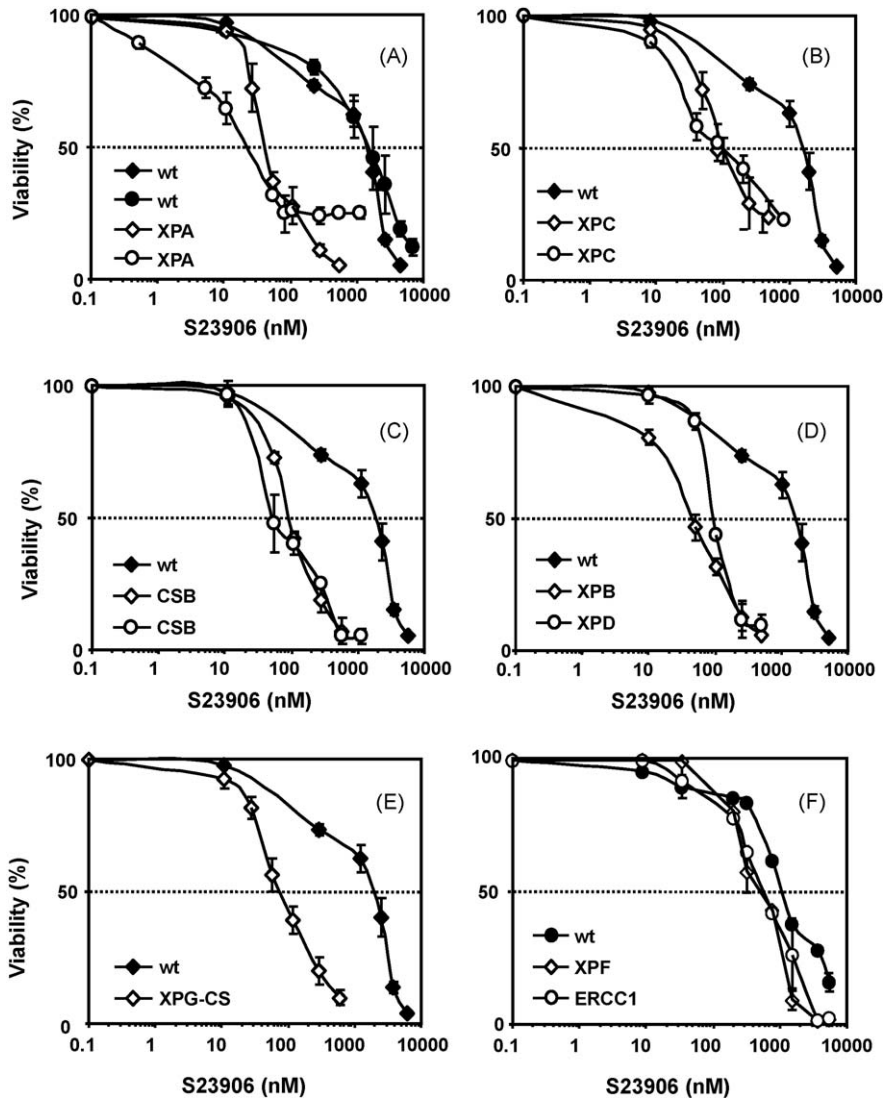

Fig. 1. Cytotoxic activity of S23906 toward NER-deficient cells. Repair-proficient and -deficient cells were exposed to the indicated concentrations of S23906 for 3–4 generation times and the growth inhibitory effect was determined by the MTT viability assay. (A) Sensitivity of XPA-deficient cells to S23906. (◆) Repair-proficient SV40-transformed MRC5-SV cells; (◇) XPA-deficient XP12RO-SV transformed cells; (●) repair-proficient 198VI primary fibroblasts; (○) XPA-deficient XP162VI primary fibroblasts. (B) Sensitivity of XPC-deficient cells to S23906. (◆) Repair-proficient MRC5-SV cells; (◇) XPC-deficient XP4PA-SV SV40-transformed cells; (○) XPC-deficient XP202VI primary fibroblasts. (C) Sensitivity of CSB-deficient cells to S23906. (◆) Repair-proficient MRC5-SV cells; (◇) CSB-deficient SC1AN-SV SV40-transformed cells; (○) CSB-deficient CS539VI primary fibroblasts. (D) Sensitivity of XPB- and XPD-deficient cells to S23906. (◆) Repair-proficient MRC5-SV cells; (◇) XPB-deficient XPCS2BA-SV SV40-transformed cells; (○) XPD-deficient XP203VI-SV SV40-transformed cells. (E) Sensitivity of XPG-deficient cells to S23906. (◆) Repair-proficient MRC5-SV cells; (◇) XPG-deficient XPCS1LV SV40-transformed cells. (F) Sensitivity of ERCC1- and XPF-deficient cells to S23906. (●) Repair-proficient 198VI primary fibroblasts; (○) ERCC1-deficient 165TOR primary fibroblasts; (◇) XPF-deficient XP871VI primary fibroblasts. All values are averages of at least two independent experiments, each done in duplicate. Standard deviations are indicated by error bars when they exceed symbol size.

primary cells. The results (Fig. 1A, circles) confirmed the marked sensitivity of XPA-deficient cells to S23906.

3.2. Cytotoxicity of S23906 toward cells deficient in XPC, CSB, XPB, XPD, XPG, ERCC1 or XPF

We then established the relative roles of the global and transcription-coupled NER pathways. XPC cells, that are deficient in global genome repair, were about 20-fold more sensitive to S23906, whereas CSB cells, that are deficient for transcription-coupled repair, were 20- to 35-fold more sensitive to S23906, compared to repair-proficient cells (Fig. 1B and C). Similar differences were observed for cells deficient in the XPB and XPD helicases (Fig. 1D) or the XPG endonuclease (Fig. 1E). In comparison, cells deficient in ERCC1 or XPF showed at the most 2- to 3-fold increased sensitivity (Fig. 1F).

3.3. Repair of S23906 adducts

To confirm that the pronounced sensitivity of XPA-deficient cells was associated with repair of S23906 adducts, immortalized cells, proficient or deficient for XPA, were exposed to different doses of S23906, and unscheduled DNA synthesis (UDS) was determined. The results show that S23906 treatment was accompanied by increased DNA repair in NER-proficient, but not in XPA-deficient cells (Fig. 2A, left panel), similar to what was observed for UV-C treatment (Fig. 2A, right panel). Therefore, the pronounced sensitivity of XPA cells is, at least in part, due to the absence of NER activity.

Next, DNA repair synthesis was determined for primary cells proficient or deficient for XPA, ERCC1 and XPF. In contrast to the XPA cells, ERCC1 and XPF cells showed residual repair activity, which was particularly marked for UV-irradiated ERCC1 cells

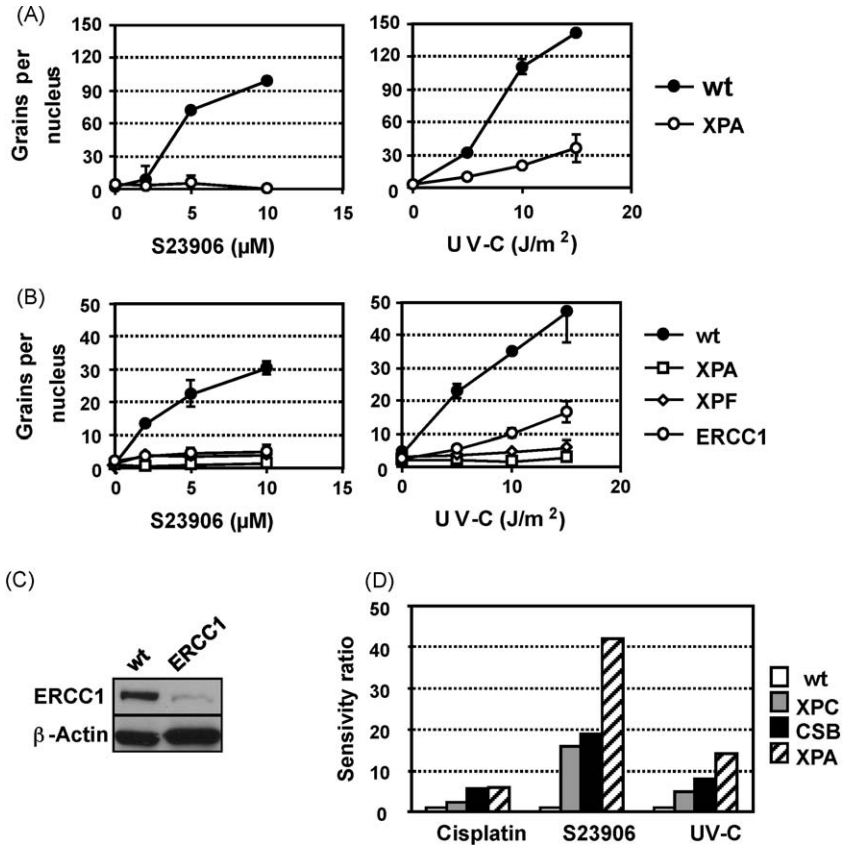

Fig. 2. Comparison of S23906 with other NER substrates. (A) Unscheduled DNA synthesis (UDS) in (●) XPA-proficient (MRC5-SV) and (○) XPA-deficient (XP12RO-SV) cells following exposure to S23906 or UV irradiation. All values are averages at least 100 individual nuclei from two independent experiments. Standard deviations are indicated by error bars when they exceed symbol size. (B) Unscheduled DNA synthesis (UDS) in (●) repair-proficient (198VI), (○) ERCC1-deficient (165TOR), (◇) XPF-deficient (XP871VI) and (□) XPA-deficient (XP162VI) primary fibroblasts following exposure to S23906 or UV irradiation. All values are averages at least 30 individual nuclei from two independent experiments. Standard deviations are indicated by error bars when they exceed symbol size. (C) Western blot analysis of ERCC1 in ERCC1-proficient wt (198VI) and ERCC1-deficient (165TOR) primary fibroblasts (lanes 1 and 2, respectively). (D) Relative sensitivities of XPC-, CSB- and XPA-deficient cells to S23906, cisplatin and UV irradiation. The cytotoxic activities of cisplatin, S23906 and UV irradiation were determined for repair-proficient MRC5-SV cells (white bars), XPC-deficient XP4PA cells (grey bars), CSB-deficient SC1AN-SV cells (black bars) and XPA-deficient XP12RO-SV cells (hatched bars) by the MTT assay. The relative sensitivity was calculated as the ratio between the IC_{50} value for the wt cells and the IC_{50} value for the indicated repair-deficient strain. A value of 1 indicates unchanged sensitivity whereas values bigger than 1 indicate the corresponding degree of increased sensitivity.

(Fig. 2B, right panel). For S23906, the residual activity of ERCC1 was less pronounced. However, it should be noted that the IC_{50} values for ERCC1- and XPF-deficient cells are in the 1 μM dose range, where the differences in UDS between repair-proficient and ERCC1- and XPF-deficient cells are less important than at higher doses of S23906.

Western blot analysis of repair-proficient and ERCC1-deficient cells (Fig. 2C, lanes 1 and 2, respectively) revealed that the ERCC1-deficient cells have very low levels of full-length ERCC1 protein. These findings indicate that there is no straightforward relationship between the protein levels and the catalytic activity of ERCC1 in these cells, in agreement with previous reports [19].

3.4. Comparison between S23906, cisplatin and UV irradiation

We then compared the impact of XPC, CSB and XPA function on the sensitivity to S23906 in comparison with two classical NER substrates, cisplatin and UV. Repair-proficient cells or cells deficient for XPC, CSB or XPA were exposed to S23906, cisplatin or UV irradiation and the IC_{50} values were determined by the MTT assay. The relative sensitivity was calculated as the ratio between the IC_{50} of the repair-proficient cells divided with the IC_{50} of the repair-deficient cells. The results (Fig. 2D) show that the 3 NER factors play a more pronounced role in the sensitivity to S23906, compared to UV irradiation and cisplatin. Both XPC and CSB were needed for the repair of UV and S23906 lesions, whereas CSB seems to be more important than XPC for cisplatin.

3.5. Influence of XPA on the induction of S23906-induced DNA strand breaks

We have previously shown that S23906 exposure is accompanied by the formation of toxic DNA strand breaks [4]. To determine if NER has an influence on the induction of strand breaks, repair-proficient and XPA-deficient cells were exposed to different doses of S23906, and the induction of DNA strand breaks was determined by single cell electrophoresis under alkaline conditions (the alkaline comet assay). The results show that XPA deficiency was accompanied by significantly ($p < 0.001$) increased formation of DNA strand breaks (Fig. 3A).

For further analysis, the induction of gamma-H2AX, a sensitive surrogate marker for the formation of double strand breaks, was determined in repair-proficient and XPA-deficient cells after 1 h exposure to S23906. The results show that XPA deficiency is accompanied by a significant ($p < 0.001$) increase in gamma-H2AX-associated fluorescence, compared to repair-proficient cells (Fig. 3B and C). Taken together, these results indicate that unrepaired S23906 adducts are converted into toxic double strand breaks, coherent with the marked influence of NER on cellular survival.

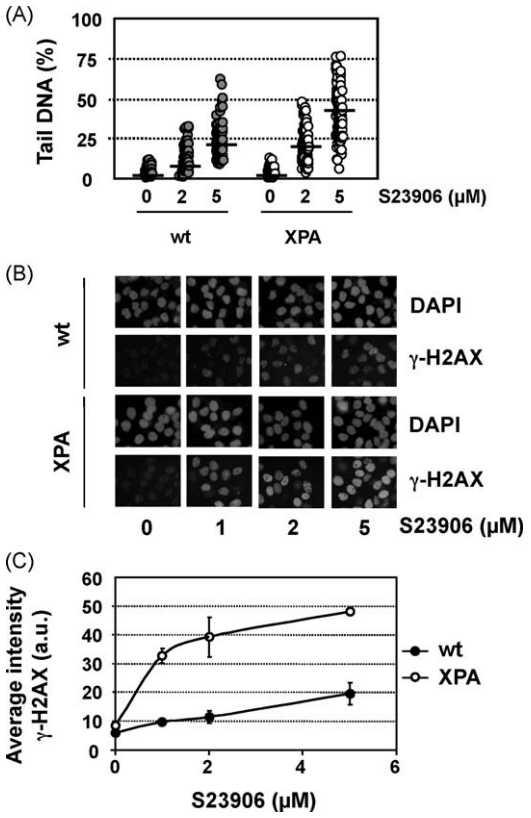

Fig. 3. S23906 exposure is accompanied by increased formation of DNA strand breaks in XPA-deficient cells. (A) (●) Repair-proficient MRC5-SV and (○) XPA-deficient XP12RO-SV cells were exposed to the indicated concentrations of S23906 for 1 h and the induction of DNA strand breaks was determined by the alkaline comet assay. The results indicate the levels of DNA damage in individual cells from a typical experiment and are expressed as the % of total DNA present in the comet tail. Bars, average levels of DNA damage. (B) Repair-proficient MRC5-SV and XPA-deficient XP12RO-SV cells were exposed to the indicated concentrations of S23906 for 1 h and the induction of phospho-H2AX was determined by immunocytochemistry. (C) (●) Repair-proficient MRC5-SV and (○) XPA-deficient XP12RO-SV cells were exposed to the indicated concentrations of S23906 for 1 h as shown in (B), and the phospho-H2AX signal was quantified by MetaMorph analysis. a.u., arbitrary units. Each point represents the average of at least 100 cells. Standard deviations are indicated by error bars when they exceed symbol size.

3.6. NER in cells with acquired S23906 resistance

We then wanted to extend our findings to a different cellular model. KB carcinoma cells were exposed to stepwise increased concentrations of S23906 in the cell culture media as previously described [4]. The resulting KB/906 cells were 15-fold resistant to S23906 and approximately 3-fold cross-resistant to both cisplatin and UV irradiation [4].

Next, UDS, which principally measures global genome repair, was determined after cellular exposure to S23906 or UV irradiation. The results showed significant increased UDS in the KB/906 cells for all treatment conditions studied (Fig. 4A) ($p < 0.001$). For further confirmation, the repair capacity of cellular extracts from parental and S23906-resistant cells toward irradiated plasmid DNA was compared. Again, extracts from KB/906 cells showed markedly higher repair activity than extracts from the parental KB cells (Fig. 4B).

To determine if transcription-coupled repair was also up-regulated, KB and KB/906 cells were UV-irradiated, and the resumption of RNA synthesis was determined by the incorporation of radiolabeled uridine. The results show that UV irradiation was accompanied by transcriptional inhibition in both cell lines. Three hours after irradiation, the transcriptional activity was fully recovered in KB/906 cells but remained depressed in the parental KB cells, which required an additional 3 h for full recovery (Fig. 4C).

3.7. Expression of NER factors in parental and S23906-resistant cells

Cellular levels of XPC, CSB, XPA and ERCC1 proteins were determined by Western blot analysis. The results showed 4- to 5-fold increased levels of XPC and CSB proteins and a 2-fold increase of XPA in the resistant KB/906 cells. In clear contrast, protein levels of ERCC1 were comparable for parental and resistant cells (Fig. 5A).

For further characterization, KB and KB/906 cells were incubated in the absence or presence of cycloheximide (10 μM), an inhibitor of de novo protein synthesis, over a 12 h period and the protein levels of XPC were determined by Western blot analysis. The results show unchanged levels of XPC protein in both cell lines over the entire 12 h period (data not shown).

Messenger RNA levels of different NER factors were determined by qRT-PCR analysis. Unexpectedly, except for XPA, a modest down-regulation was observed for most XP factors in KB/906 cells, compared to the parental cells (Fig. 5B).

3.8. ERCC1 codon 118 polymorphism in parental and S23906-resistant cells

The ERCC1 gene exists in several polymorphisms, among which the polymorphism in codon 118 may be particularly important for resistance to alkylating agents [25]. PCR amplification and sequencing of codon 118 in parental and S23906-resistant cells showed that both cell lines presented the same sequence corresponding to the rs11615, N118N (T354C) polymorphism with C present on both alleles. Therefore, S23906 selection was not accompanied by mutations at codon 118 of ERCC1.

3.9. Recruitment of ERCC1 in parental and S23906-resistant cells

Next, the recruitment of ERCC1 to locally UV-irradiated sites was determined. The results show that ERCC1 is recruited to foci with 6-4 photoproducts (6-4PPs) in both parental (Fig. 5C, left) and S23906-resistant cells (Fig. 5C, right). These findings suggest that the recruitment of XPF/ERCC1 proceeds normally in both cell lines.

4. Discussion

We here describe the interaction of the bulky monofunctional antitumor alkylator S23906 with the nucleotide excision repair machinery. Characterization of patient-derived NER-deficient primary or immortalized fibroblast cell lines unambiguously shows that S23906 adducts are recognized by GG-NER as well as by TC-NER. Deficiencies of all NER proteins tested (XPC, CSB, XPD, XPB, XPG, XPA, ERCC1 and XPF) were accompanied by increased sensitivity to S23906, which for cells deficient in XPC, CSB and XPA clearly exceeded the sensitivity levels observed for UV and cisplatin, two classical NER substrates. Although patient-derived XP mutants have the advantage of being clinically relevant, they are derived from different individuals and are therefore not isogenic. Thus, all findings for wt, CSB, XPC and ERCC1–XPF cells were independently confirmed using cells derived from two different individuals. For XPC cells, we were even able to compare the response of cells from 2 different individuals carrying the same mutation. For further confirmation, all findings for S23906 were compared with the response to the classical NER substrates UV radiation and cisplatin, which gave a response coherent with the literature.

It is intriguing that the sensitivity pattern of S23906 is very different from the pattern of yondelis, another bulky alkylating agent that binds to the minor groove of DNA at the same residue as

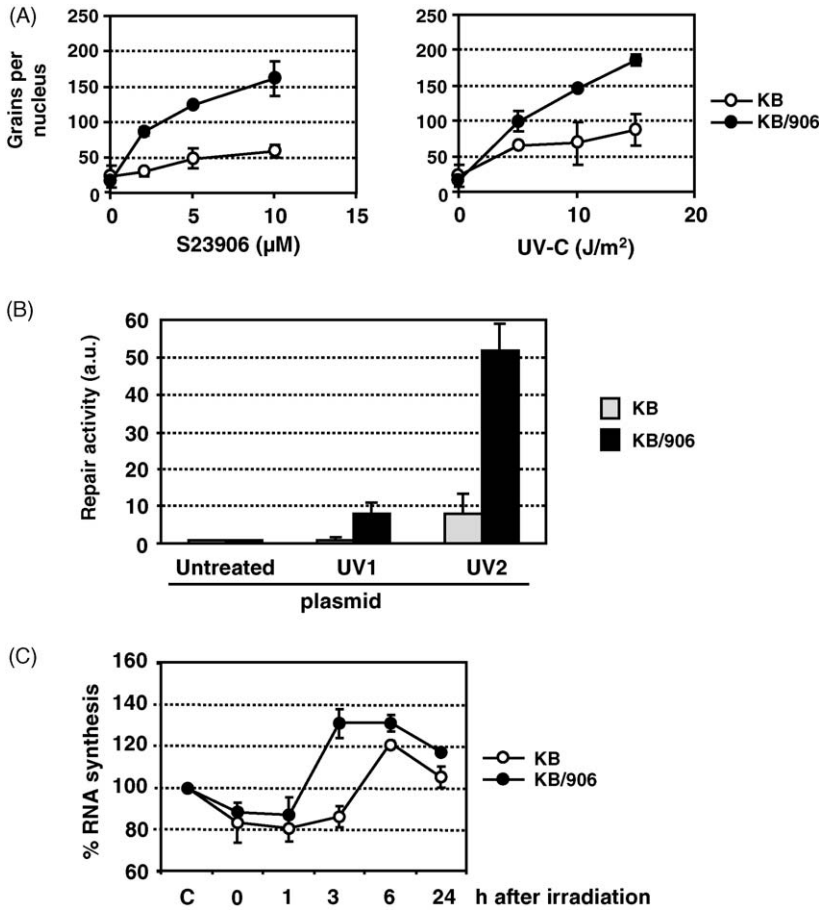

Fig. 4. Increased NER activity in cells acquired S23906 resistance. (A) Parental (○) and S23906-resistant (●) KB cells were exposed to the indicated doses of S23906 or UV-C for 3 h in the presence of radiolabeled thymidine, and the NER activity was determined by UDS. (B) Nuclear extracts from parental and resistant KB cells were incubated in the presence of UV-C modified plasmids (UV1: 200 J/m^2 and UV2: 800 J/m^2), and the NER activity was determined by the incorporation of digoxigenylated deoxynucleotide monophosphates. The columns show the differences in repair activity between UV-modified and untreated plasmids. Standard deviations are indicated by error bars. a.u., arbitrary units. (C) Transcriptional recovery of parental (○) and resistant (●) KB cells. Cells were exposed to 15 J/m^2 of UV-C, followed by post-incubation for the indicated times. Transcriptional activity was determined by the incorporation of radiolabeled uridine, followed by scintillation counting. Standard deviations are indicated by error bars when they exceed symbol size.

S23906. In contrast to S23906, Yondelis adducts are not recognized by GG-NER [17]. Furthermore, the yondelis adducts are not removed by NER, but rather converted into stable complexes composed of the DNA adduct and the XPG endonuclease [18]. The most striking difference between S23906 and yondelis adducts is their influence on the surrounding DNA. S23906 adducts have a helicase-like activity that destabilize local base-pairing whereas yondelis adducts act as cross-link mimetics that stabilize the local duplex structure. This suggests that the influence of DNA adducts on the local DNA conformation have major impact on their subsequent processing by the NER pathway.

We then extended our studies to a different model system, KB carcinoma cells with acquired resistance to S23906. These cells showed increased NER activity *in vivo* as well as toward damaged plasmid DNA *in vitro*. Importantly, both global genome NER, as shown by unscheduled DNA synthesis, and transcription-coupled NER, as shown by transcriptional recovery, were up-regulated in the S23906-resistant cells. The increased NER activity was accompanied by an important accumulation of XPC, CSB and, to a lesser degree, XPA proteins, but not of their respective mRNAs, possibly due to negative feedback control. Incubation with cycloheximide, an inhibitor of de novo protein synthesis, was not accompanied by any detectable modifications of the XPC levels in parental or S23906-resistant KB cells, similar to what has been reported for primary human fibroblasts [26]. These findings suggest, that the parental and resistant cell lines have similar stability/turn-over of the XPC protein.

The importance of XPC was unexpected, considering that irofulven and yondelis adducts are not recognized by GG-NER. However, an important role for XPC in the recognition and repair of S23906 adducts is fully coherent with current models for the XPC recognition of damaged DNA. In particular, it has been shown that the initial recognition of damaged DNA by the XPC orthologue Rad4 as well as by human XPC requires a thermodynamically destabilized double helix with non-hydrogen bonded bases. Subsequently, a stable recognition complex is formed, mediated by binding of the beta-hairpin domain 3 (BHD3) of XPC to single-stranded DNA [27,28]. These observations strongly suggest that the "helicase"-like influence of the S23906 adducts on the local duplex structure favors their recognition by XPC.

No alterations were observed for ERCC1 on neither the DNA, RNA or protein levels nor at the functional level in the S23906-resistant cells in spite of their increased NER activity. This was unexpected considering the current use of ERCC1 in response prediction to platinum-based therapies. There are two major models to explain the role of ERCC1 in response prediction. First, ERCC1 is classically considered as a biomarker for NER activity [11,29]. Considering that the NER pathway requires a large number of proteins, the predictive value of ERCC1 could be explained by (a) a specific role of ERCC1, with ERCC1 protein levels being the rate-

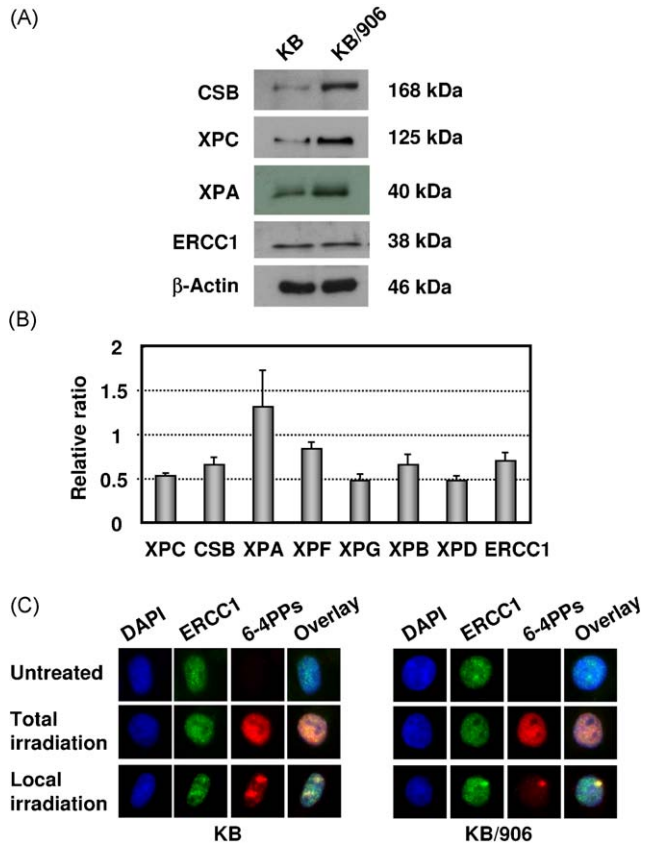

Fig. 5. NER expression and recruitment in parental and resistant KB cells. (A) Expression of CSB, XPC, XPA and ERCC1 proteins in parental and resistant KB cells was determined by Western blot analysis with beta-actin as loading control. (B) Expression of mRNA for XPC, CSB, XPA, XPF, XPG, XPB, XPD and ERCC1 was determined by quantitative RT-PCR and normalized using the geometric mean of the three reference genes, beta-actin, HMBS and GAPDH. The columns represent the relative expression of the indicated NER factors in S23906-resistant cells compared to the parental cells. Unchanged expression levels correspond to 1. Standard deviations are indicated by error bars. (C) Parental KB cells and resistant KB/906 cells were exposed to 150 J/m^2 in the presence or absence of a filter with micropores (5 μm). After 1 h post-incubation, the recruitment of ERCC1 to 6-4 photoproduct was observed by immunochemistry.

limiting factor for the overall NER pathway or, alternatively, (b) a representative role for ERCC1, which would be the case if the expression of the different NER proteins, including, but not restricted to, ERCC1, was coordinated.

An alternative, more recent model suggests that ERCC1 is predictive because it is a multifunctional protein involved in different pathways needed for the repair of platinum adducts [12]. ERCC1–XPF (but not other NER proteins) is required for incision of cross-linked DNA [30,31] as well as for two different types of error-prone DSB repair, single-strand annealing [32] and microhomology-mediated end joining [33]. ERCC1–XPF also participates in the Fanconi anemia pathway during homologous recombination [34] and is associated with telomeres, where it modulates recombination of telomeric sequences and loss of telomeres from unprotected chromosome ends [35,36]. This is important, since cisplatin forms a wide range of DNA lesions including monofunctional adducts, intrastrand cross-links, interstrand cross-links and likely interferes with telomeric functions [37]. Therefore, it is possible, that ERCC1–XPF expression may be rate-limiting for some function, other than NER, needed for repair of platinum adducts.

The results presented here clearly come out in favor of the second model and indicate that there is no straightforward relationship between protein levels of ERCC1 and NER activity. Specifically, the patient-derived ERCC1-mutated 165TOR cells showed only modest levels of increased sensitivity to S23906 in spite of strongly decreased ERCC1 protein levels similar to the findings reported for ERCC1-deficient cells exposed to UV irradiation [19]. Furthermore, cells with acquired resistance to S23906 show increased NER activity but unchanged ERCC1 levels. Together, these findings suggest that although ERCC1–XPF is a necessary element of the NER pathway and needed for repair of S23906 adducts, it is not rate-limiting, consistent with its functions in the last, rather than the initial steps, of the NER pathway. It is possible that the catalytic activity of ERCC1 is sufficiently high to carry out the excision step even at low protein levels. Alternatively, the last excision step might, at least in part, also be carried out by a FLAP endonuclease like FEN1.

In conclusion, ERCC1 expression cannot be recommended for the prediction of sensitivity to bulky monofunctional alkylators like S23906, whereas XPC and CSB appear as attractive candidates. Generally, ERCC1 expression is not a marker of NER activity, but may be correlated with the additional activities of this multifunctional protein in recombination and cross-link repair.

Acknowledgements

This work was supported by Cancer Research and Drug Discovery, Institut de Recherches Servier, Croissy sur Seine, France; by CAPES/COFECUB [French-Brazilian Collaborative Research Grant No. 583/07]; and by Institut National de Cancer [CETIRICOL, PL06.008]. Daniele Grazziotin Soares was supported by the Association pour la Recherche sur le Cancer (ARC) Villejuif, France. The contribution of Patrick Calsou and Bernard Salles (Institut de Pharmacologie et de Biologie Structurale, Toulouse) for the 3D assay and of Patrick Saulier (Institut Gustave-Roussy, Villejuif) for the determination of the ERCC1 polymorphism is gratefully acknowledged.

References

[1] David-Cordonnier MH, Laine W, Lansiaux A, Rosu F, Colson P, de Pauw E, et al. Covalent binding of antitumor benzoacronycines to double-stranded DNA induces helix opening and the formation of single-stranded DNA: unique consequences of a novel DNA-bonding mechanism. Mol Cancer Ther 2005;4:71–80.
[2] David-Cordonnier MH, Lainé W, Lansiaux A, Kouach M, Briand G, Pierré A, et al. Alkylation of guanine in DNA by S23906-1, a novel potent antitumor compound derived from the plant alkaloid acronycine. Biochemistry 2002;41:9911–20.
[3] Nguyen QC, Nguyen TT, Yougnia R, Gaslonde T, Dufat H, Michel S, et al. Acronycine derivatives: a promising series of anticancer agents. Anticancer Agents Med Chem 2009;9:804–15.
[4] Léonce S, Kraus-Berthier L, Golsteyn RM, David-Cordonnier MH, Tardy C, Lansiaux A, et al. Generation of replication-dependent double-strand breaks by the novel N2-G-alkylator S23906-1. Cancer Res 2006;66:7203–10.
[5] Soares DG, Escargueil AE, Poindessous V, Sarasin A, de Gramont A, Bonatto D, et al. Replication and homologous recombination repair regulate DNA double-strand break formation by the antitumor alkylator ecteinascidin 743. Proc Natl Acad Sci U S A 2007;104:13062–7.
[6] Cahuzac N, Studény A, Marshall K, Versteege I, Wetenhall K, Pfeiffer B, et al. An unusual DNA binding compound S23906, induces mitotic catastrophe in cultured human cells. Cancer Lett)2009;(September 14) [Epub ahead of print].
[7] Hoeijmakers JH. Genome maintenance mechanisms for preventing cancer. Nature 2001;411:366–74.
[8] Volker M, Moné MJ, Karmakar P, van Hoffen A, Schul W, Vermeulen W, et al. Sequential assembly of the nucleotide excision repair factors in vivo. Mol Cell 2001;8:213–24.
[9] Riedl T, Hanaoka F, Egly JM. The comings and goings of nucleotide excision repair factors on damaged DNA. EMBO J 2003;22:5293–303.
[10] Hanawalt PC, Spivak G. Transcription-coupled DNA repair: two decades of progress and surprises. Nat Rev Mol Cell Biol 2008;9:958–70.
[11] Olaussen KA, Dunant A, Fouret P, Brambilla E, André F, Haddad V, et al. DNA repair by ERCC1 in non-small-cell lung cancer and cisplatin-based adjuvant chemotherapy. N Engl J Med 2006;355:983–91.
[12] Bhagwat NR, Roginskaya VY, Acquafondata MB, Dhir R, Wood RD, Niedernhofer LJ. Immunodetection of DNA repair endonuclease ERCC1–XPF in human tissue. Cancer Res 2009;69:6831–8.
[13] Jaspers NG, Raams A, Kelner MJ, Ng JM, Yamashita YM, Takeda S, et al. Anti-tumour compounds illudin S and Irofulven induce DNA lesions ignored by

global repair and exclusively processed by transcription- and replication-coupled repair pathways. DNA Repair (Amst) 2002;1:1027–38.
[14] Koeppel F, Poindessous V, Lazar V, Raymond E, Sarasin A, Larsen AK. Irofulven cytotoxicity depends on transcription-coupled nucleotide excision repair and is correlated with XPG expression in solid tumor cells. Clin Cancer Res 2004;10:5604–13.
[15] Escargueil AE, Poindessous V, Soares DG, Sarasin A, Cook PR, Larsen AK. Influence of irofulven, a transcription-coupled repair-specific antitumor agent, on RNA polymerase activity, stability and dynamics in living mammalian cells. J Cell Sci 2008;121:1275–83.
[16] Poindessous V, Koeppel F, Raymond E, Comisso M, Waters SJ, Larsen AK. Marked activity of irofulven toward human carcinoma cells: comparison with cisplatin and ecteinascidin. Clin Cancer Res 2003;9:2817–25.
[17] Damia G, Silvestri S, Carrassa L, Filiberti L, Faircloth GT, Liberi G, et al. Unique pattern of ET-743 activity in different cellular systems with defined deficiencies in DNA-repair pathways. Int J Cancer 2001;92:583–8.
[18] Herrero AB, Martín-Castellanos C, Marco E, Gago F, Moreno S. Cross-talk between nucleotide excision and homologous recombination DNA repair pathways in the mechanism of action of antitumor trabectedin. Cancer Res 2006;66:8155–62.
[19] Jaspers NG, Raams A, Silengo MC, Wijgers N, Niedernhofer LJ, Robinson AR, et al. First reported patient with human ERCC1 deficiency has cerebro-oculo-facio-skeletal syndrome with a mild defect in nucleotide excision repair and severe developmental failure. Am J Hum Genet 2007;80:457–66.
[20] Olive PL, Banáth JP. The comet assay: a method to measure DNA damage in individual cells. Nat Protoc 2006;1:23–9.
[21] Mori T, Nakane M, Hattori T, Matsunaga T, Ihara M, Nikaido O. Simultaneous establishment of monoclonal antibodies specific for either cyclobutane pyrimidine dimer or (6-4)photoproduct from the same mouse immunized with ultraviolet-irradiated DNA. Photochem Photobiol 1991;54:225–32.
[22] Salles B, Provot C, Calsou P, Hennebelle I, Gosset I, Fournié GJ. A chemiluminescent microplate assay to detect DNA damage induced by genotoxic treatments. Anal Biochem 1995;232:37–42.
[23] Pencreach E, Guérin E, Nicolet C, Lelong-Rebel I, Voegeli AC, Oudet P, et al. Marked activity of irinotecan and rapamycin combination toward colon cancer cells in vivo and in vitro is mediated through cooperative modulation of the mammalian target of rapamycin/hypoxia-inducible factor-1alpha axis. Clin Cancer Res 2009;15:1297–307.
[24] Vandesompele J, De Preter K, Pattyn F, Poppe B, Van Roy N, De Paepe A, et al. Accurate normalization of real-time quantitative RT-PCR data by geometric averaging of multiple internal control genes. Genome Biol 2002. 33:research 0034.1-0034.11.
[25] Viguier J, Boige V, Miquel C, Pocard M, Giraudeau B, Sabourin JC, et al. ERCC1 codon 118 polymorphism is a predictive factor for the tumor response to oxaliplatin/5-fluorouracil combination chemotherapy in patients with advanced colorectal cancer. Clin Cancer Res 2005;11:6212–7.
[26] Yasuda G, Nishi R, Watanabe E, Mori T, Iwai S, Orioli D, et al. In vivo destabilization and functional defects of the xeroderma pigmentosum C protein caused by a pathogenic missense mutation. Mol Cell Biol 2007;27:6606–14.
[27] Min JH, Pavletich NP. Recognition of DNA damage by the Rad4 nucleotide excision repair protein. Nature 2007;449:570–5.
[28] Camenisch U, Träutlein D, Clement FC, Fei J, Leitenstorfer A, Ferrando-May E, et al. Two-stage dynamic DNA quality check by xeroderma pigmentosum group C protein. EMBO J 2009;28:2387–99.
[29] Gossage L, Madhusudan S. Current status of excision repair cross complementing-group 1 (ERCC1) in cancer. Cancer Treat Rev 2007;33:565–77.
[30] McHugh PJ, Spanswick VJ, Hartley JA. Repair of DNA interstrand crosslinks: molecular mechanisms and clinical relevance. Lancet Oncol 2001;2:483–90.
[31] Niedernhofer LJ, Odijk H, Budzowska M, van Drunen E, Maas A, Theil AF, et al. The structure-specific endonuclease ERCC1–XPF is required to resolve DNA interstrand cross-link-induced double-strand breaks. Mol Cell Biol 2004;24:5776–87.
[32] Al-Minawi AZ, Saleh-Gohari N, Helleday T. The ERCC1/XPF endonuclease is required for efficient single-strand annealing and gene conversion in mammalian cells. Nucleic Acids Res 2008;36:1–9.
[33] Ahmad A, Robinson AR, Duensing A, van Drunen E, Beverloo HB, Weisberg DB, et al. ERCC1–XPF endonuclease facilitates DNA double-strand break repair. Mol Cell Biol 2008;28:5082–92.
[34] Bhagwat N, Olsen AL, Wang AT, Hanada K, Stuckert P, Kanaar R, et al. XPF–ERCC1 participates in the Fanconi anemia pathway of cross-link repair. Mol Cell Biol 2009;29:6427–37.
[35] Zhu XD, Niedernhofer L, Kuster B, Mann M, Hoeijmakers JH, de Lange T. ERCC1/XPF removes the 3′ overhang from uncapped telomeres and represses formation of telomeric DNA-containing double minute chromosomes. Mol Cell 2003;12:1489–98.
[36] Muñoz P, Blanco R, Flores JM, Blasco MA. XPF nuclease-dependent telomere loss and increased DNA damage in mice overexpressing TRF2 result in premature aging and cancer. Nat Genet 2005;37:1063–71.
[37] Ishibashi T, Lippard SJ. Telomere loss in cells treated with cisplatin. Proc Natl Acad Sci U S A 1998;95:4219–23.